Corporate Office

FINAL REPORT

Fabrication and Evaluation of Superconducting and Semiconducting Materials

SFA, Inc. ■ 1401 McCormick Drive ■ Landover, Maryland 20785-5322 ■ Tel. (301) 925-9400 ■ Fax (301) 925-8612

SECURITY CLASSIFICATION: Unclassified

SFA--93/003

Fabrication and Evaluation of Superconducting and Semiconducting Materials

Prepared by: William Lechter

SFA, Inc.
1401 McCormick Drive
Landover, Maryland 20785

Date: September 1993

Contract Number: N00014-89-C-2392

Prepared for: Naval Research Laboratory
4555 Overlook Avenue, SW
Washington, DC 20375-5000

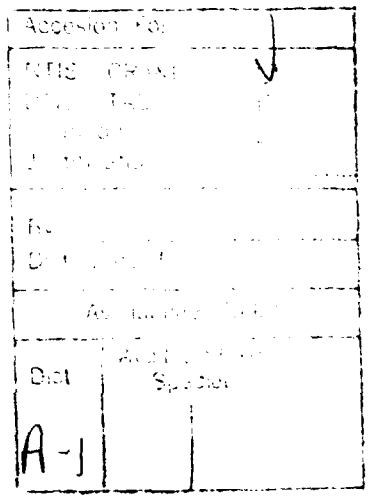

REPORT DOCUMENTATION PAGE

Form Approved
OMB No. 0704-0188

1. AGENCY USE ONLY (*Leave Blank*)	2. REPORT DATE	3. REPORT TYPE AND DATES COVERED
	September 1993	Final Report 9/30/89 to 6/15/93

4. TITLE AND SUBTITLE
Fabrication and Evaluation of Superconducting and Semiconducting Materials

5. FUNDING NUMBERS
N00014-89-C-2392

6. AUTHOR(S)
William Lechter

7. PERFORMING ORGANIZATION NAME(S) AND ADDRESS(ES)
SFA, Inc.
1401 McCormick Drive
Landover, MD 20785

8. PERFORMING ORGANIZATION REPORT NUMBER
SFA--93/003

9. SPONSORING/MONITORING AGENCY NAME(S) AND ADDRESS(ES)
Naval Research Laboratory
4555 Overlook Ave., SW
Washington, DC 20375-5000

10. SPONSORING/MONITORING AGENCY REPORT NUMBER

11. SUPPLEMENTARY NOTES

12a. DISTRIBUTION/AVAILABILITY STATEMENT

12b. DISTRIBUTION CODE

13. ABSTRACT (*Maximum 200 words*)

SFA provided research support to the Naval Research Laboratory Material Physics Branch by conducting investigations into the properties of superconducting, magnetic, and other solid state materials. Studies were made with an assortment of experimental techniques, including sophisticated materials preparation, magnetic resonance, electrical resistivity, magnetic susceptibility, the Mossbauer effect, and a variety of other techniques that probe the physical state of matter. SFA also aided the Material Physics Branch in conducting research into applied problems such as the design of magnetic shielding and superconducting quantum interference device (SQUID) magnetometry detection of magnetic anomalies. SFA provided research assistance in the areas of bulk ceramic sample preparation, conversion electron Mossbauer spectrometry, ultra-high vacuum thin film deposition and characterization, sputter thin film deposition, and superconducting measurements

14. SUBJECT TERMS	15. NUMBER OF PAGES	16. PRICE CODE
	24 pages	

17. SECURITY CLASSIFICATION OF REPORT	18. SECURITY CLASSIFICATION OF THIS PAGE	19. SECURITY CLASSIFICATION OF ABSTRACT	20. LIMITATION OF ABSTRACT
Unclassified	Unclassified	Unclassified	Unlimited

Introduction

Under contract N00014-89-C-2392, SFA provided research support to the Naval Research Laboratory Material Physics Branch by conducting investigations into the properties of superconducting, magnetic, and other solid state materials. Studies were made with an assortment of experimental techniques, including sophisticated materials preparation, magnetic resonance, electrical resistivity, magnetic susceptibility, the Mossbauer effect, and a variety of other techniques that probe the physical state of matter. SFA also aided the Material Physics Branch in conducting research into applied problems such as the design of magnetic shielding and superconducting quantum interference device (SQUID) magnetometry detection of magnetic anomalies.

SFA conducted research and provided research assistance in the following areas:

- Bulk Ceramic Sample Preparation
- Conversion Electron Mossbauer Spectrometry
- Ultra-High Vacuum Thin Film Deposition and Thin Film Characterization
- Sputter Thin Film Deposition
- Superconducting Measurements

Bulk Ceramic Sample Preparation

SFA manufactured bulk ceramic samples by preparing the necessary ingredient chemicals and weighing the reagents on an analytical balance to the proper mass for the stochiometrical correct structure. The mixture of powdered chemicals were then milled to produce fine powders (10–20 microns), after which the powder was processed. SFA processed the chemicals through a prescribed temperature and atmosphere cycle.

SFA also carried out X-ray diffraction measurements on the prepared samples to permit verification of the desired structures. SFA made the necessary X-ray measurements to determine the reaction of chemicals, structure of materials, and phase of the sample. The X-ray data was interpreted to determine the purity of the sample and to identify the material.

Conversion Electron Mossbauer Spectrometry

SFA assembled and maintained a conversion electron Mossbauer spectrometer using a cylindrical mirror analyzer with computer controlled temperatures, depth selection, and data acquisition. SFA personnel developed software as needed to perform data analysis and to control the system. SFA maintained equipment and designed hardware to perform desired functions.

SFA performed original research using conversion electron Mossbauer spectrometry on such iron-based materials as thin films, fine particles, amorphous alloys, and single crystals. SFA personnel prepared samples for measurement and analyzed data in accordance with current theories concerning the origin and distribution of iron hyperfine fields and amorphous alloys, single crystals, and surfaces.

Ultra-High Vacuum Thin Film Deposition and Thin Film Characterization

SFA personnel fabricated thin films, and characterized and analyzed their properties for such applications as magneto-resistive sensors. SFA also maintained the high-vacuum thin film deposition equipment belonging to the Material Physics Branch, and measured the thickness of thin films with a Dektak profilometer. The films must have a sharp boundary between the deposited area and bare substrate to obtain optimal results with

this technique. Sharp edges were produced by an acid etching procedure. The section of the film that was not to be etched was first coated with an acid-resistant material. It was found that the simplest, quickest, and least expensive etch-resist is household contact cement. An etch consisting of a mixture of nitric, hydrochloric, and hydrofluoric acids was developed by trial and error on test films that provided rapid removal of the deposited film, but did not damage the substrate or seep under the etch resist material. Prior to each batch of profilometer measurements, the instrument was turned on and allowed to stabilize for a minimum of two hours, and the room temperature lowered to 64°F to reduce temperature fluctuations caused by the cycling of the air conditioner. The instrument's accuracy was checked by measuring a certified thickness standard. Each film was measured at least three times, in different locations, to check for any unusual film inhomogeneities.

Resistance measurements performed by SFA personnel initially employed a four-probe Van der Pauw method on the as-deposited films. It was found that the films were very thin and of high resistance, causing this method to be too sensitive to inhomogeneity near the edges of the deposits. To avoid this problem, narrow strip patterns in the shape of the letter "H" were scratched into the films with a diamond-tipped scribe, and four copper wires were indium-soldered directly to the film at the ends of the strips. The four-probe measurement was then performed using the copper wires at contact points. The dimensions of the strips were measured with a precision of 0.1 millimeter using a magnifying comparator. Tests were performed on strip patterns of various sizes; several strips were deliberately distorted to ensure that this method was not sensitive to minor flaws in the scratched patterns. Absolute values of the resistances could be obtained via this method with a precision of 5 percent.

SFA personnel performed X-ray fluorescence composition determinations, which involved measuring the X-ray spectra of iron and silicon in the sample material. The resulting data were converted to concentrations by a calculation that required an independent calibration to set the values of a number of instrumental and sample-dependent parameters. To obtain concentrations from X-ray fluorescence data, it is necessary to first measure standard samples with known compositions and thicknesses that are identical in size and shape to the unknown specimens and are mounted in the instrument in an identical manner. For the iron-silica project, special standard samples of bulk pure iron and fused quartz were made with the same dimensions as the film specimens. The concentration calibration was based on measurements of these standards, corrected for their thickness and X-ray absorption coefficients. The calibration was tested by analyzing certified absorption standards of iron and silicon monoxide and by measuring pure iron films. To eliminate errors that may have occurred as a result of sample placement in the fluorescence instrument, special holders were designed and machined to allow reproducible specimen placement within 0.005 inch. Data were acquired on each sample to ensure statistical precision of 1 percent. Extraneous contributions to the measured signal were subtracted by numerical modeling of the background signal and by direct subtraction of bare substrate spectra. In a few cases where the two methods differed by more than a few percent, the film was remeasured and reanalyzed. The absolute accuracy of the technique developed was estimated at 5 percent, and the measurement precision was 2 percent.

Transmission electron spectroscopy examinations were performed on several films selected to represent three main composition ranges of interest. The crystalline structure of the iron phase in the films was verified to be alpha-iron by measuring and analyzing the electron diffraction patterns. Bright-field transmission electron micrographs were obtained with a magnification of up to 200,000 and a resolution of approximately 0.5 nm, nearly the limit of the instrument's capability. These micrographs were used to measure the distributions of sizes and to study the shapes of the small iron particles in the composite material. On each film, several different regions of the deposit were examined to ensure that the final micrographs correctly represented average film properties.

SFA personnel studied magnetic bilayers and multilayers and their properties, and found that magnetic multilayers with antiferromagnetic coupling between layers exhibit "spin-flop" phase transitions that may be exploited for application in magnetoresistive devices. SFA specifically studied gadolinium$_x$-iron$_{1-x}$ and gadolinium$_y$-iron$_{1-y}$ because of the relative simplicity of the structures when the layers are in the amorphous state.

This structural simplicity allows the production of simple and meaningful models of the magnetic properties of such films. The magnetic measurements were made from 4.2 to 300 K in a SQUID magnetometer with a maximum field of 55 kOe and in a vibrating-sample magnetometer with a maximum field of 90 kOe. The structures of the films were studied by large- and small-angle X-ray diffraction, and the compositions were checked with energy-dispersive X-ray fluorescence and Auger depth profiling. Spin-flop transitions were observed and attributed to the antiferromagnetic exchange coupling at the interfaces. These films also displayed novel magnetic behavior that can be explained by the enhancement of magnetostatic effects.

SFA personnel evaporated iron-copper-cobalt and iron-silver-cobalt thin-film sandwiches onto glass, silicon, and quartz substrates. The magnetic and transport properties of these samples were studied as a function of layer thickness (20A–250A) and substrate temperature during deposition (100°C–250°C). In the iron-copper-cobalt system, the two ferromagnetic films had different coercivities for a range of deposition temperatures and layer thicknesses.

SFA personnel also performed resistivity measurements as a function of temperature (1–300 K) and magnetic field (0–10 T) on antiferromagnetically coupled iron-chromium-iron sandwiches. MBE-grown sandwiches deposited epitaxially on the zinc-selenium surface and evaporated polycrystalline sandwiches deposited on glass substrates were both studied.

Sputter Thin Film Deposition

SFA personnel operated and maintained the Materials Physics Branch's sputter deposition facility. SFA deposited thin films, measured their magnetic properties, and provided data on film composition, resistivity, and microstructure. SFA personnel studied several metal-insulator composite materials, including iron-silica, iron-boron nitride, and iron-iron oxide. The desired result of the research was the development of metal-insulator composite materials with both electrical resistivity and narrow ferromagnetic resonance linewidths. Six iron-silica composite films were produced that had a constant thickness of approximately 5 nm and compositions ranging from 30 to 100 percent iron by volume. The microstructures of the films were examined by transmission electron microscopy to determine the physical nature of the phase-separation. The characterized films were then submitted for ferromagnetic resonance measurements.

The procedures used for sputter deposition were as follows:

- To optimize reproducibility and to reduce the number of adjustable parameters, all deposition parameters were kept fixed at carefully selected values, except for the power applied to the iron sputtering source and the exposure time.
- Substrate temperature was fixed at 100°C. This was low enough to avoid annealing-induced disturbance of the film properties, but high enough to ensure that the temperature could be precisely controlled.
- Substrate rotation was two rotations per second to ensure film homogeneity. This speed was selected because the net increment of thickness would be less than one atomic layer per revolution, which prevented the propagation of columnar structures.
- Silica radio frequency (RF) power was established at 500 watts because previous experience showed that occasional RF interference with other equipment occurred intermittently at higher power levels.
- Argon gas pressure was 6 milliTorr, a standard setting that was originally selected to be approximately in the middle of the stability envelope of the sputter sources.
- A background vacuum of 1×10^{-7} Torr or better was established prior to deposition. This value was selected because it was the best that could be routinely achieved with an overnight pump-down.
- Iron sputtering power varied according to desired film composition.

- Exposure time varied to obtain constant film thickness of 5 nm.

Steps used to ensure composition and thickness control were as follows:

- Initially, several films were deposited using rough guesses for the iron sputtering powers that would give the desired concentration range. Exposure times of 20 minutes or longer were used to obtain films of at least 200 nm thickness, which ensured thickness measurements with at least 10 percent accuracy.
- The compositions and thicknesses of the test films were measured.
- The results of the measurements were used to construct a "system calibration," i.e., graphs and tables of the measured deposition rates and film compositions versus the iron sputtering power.
- The system calibration was used to estimate the iron sputtering power and exposure times that would result in films of the desired composition and thickness.
- The composition and thickness of each new film was measured, and these data were used to refine the system calibration. Ultimately, the deposition parameters could be selected with enough accuracy to produce films within 5 percent of a specified composition.

Procedures used to operate and maintain the sputter deposition facility were as follows:

- Prior to each film deposition run, the interior of the vacuum chamber was cleaned of loose flakes or other debris that might have interfered with the stability of the sputtering sources or might have contaminated the films. This cleaning operation often required that the covers of the sputter sources be removed for access to locations in the source where thick deposits accumulated. Accumulations of material that were in danger of peeling or causing electrical shorts in the sources were removed by abrasion or scraping. All loose material was then vacuumed, and the sputter sources were reassembled and tested for electrical shorts. The vacuum chamber windows were cleaned by acid etching, if necessary, to allow an unobstructed view of the interior of the chamber. The demountable vacuum seal was cleaned, and fresh vacuum sealing grease applied. Finally, the substrates for the intended deposition run were installed, and the chamber was sealed. Personnel performed all operations within the vacuum chamber while wearing sterile gloves to prevent accidental contamination of the system with dirt or grease. Respirator masks and safety glasses were worn during the cleaning operation as a safety precaution against any airborne dust.
- The pumpdown procedure was then initiated. The initial stages of the sequence were automatically controlled, but required monitoring until the high vacuum valve opened. When that occurred, heating elements on the chamber were turned on to heat the chamber to approximately 50°C to facilitate the removal of condensed water vapor within the chamber. The system was left in this condition for several hours until the vacuum reached approximately 1×10^{-6} Torr. The substrate heater was then turned on and allowed to heat the substrates to approximately 300°C for a few minutes to outgas the substrates before being set at the desired substrate temperature for the deposition run. The system was left in this configuration until the vacuum reached 5×10^{-7} Torr, typically overnight. Residual gas analysis was performed to check that no unusual contamination of the vacuum existed. The Meissner coil was then cooled to pump residual water vapor, and the chamber heating elements were turned off. When the desired base pressure of 1×10^{-7} Torr was reached, another residual gas analysis was performed.
- When the base vacuum was reached, the system was prepared for the deposition run. Cooling water to the sputtering sources was turned on, and the argon sputtering gas flow initiated. The sputtering sources were turned on, and the specified deposition parameters established. The system was allowed to operate in this mode for at least five minutes to eliminate any surface contamination present on the sputtering sources and to ensure that all deposition parameters were suitable. The actual deposition of the film then consisted of simply opening the substrate shutter for the specified length of time.
- After deposition was complete, the sputtering sources, argon flow, and substrate heater were turned off. The sputter source cooling water was continued for at least 15 minutes before being turned off. The sys-

tem was maintained in the high-vacuum pumping mode until the substrate temperature dropped to 30°C or below. The Meissner coil was then defrosted and the chamber vented to atmospheric pressure using water- and oil-free nitrogen gas to avoid condensation in the chamber. Samples were recovered, and the process was repeated for the next run.

On the occasion when an equipment failure occurred, action was necessary to return the facility to working order. In addition to dealing with failures, periodic maintenance and adjustments were performed, and occasional upgrades implemented. SFA rebuilt the cryostat expander head of the cryopump, upgraded the insulation of conductors, and shielded the crystal monitor cables in the E-beam because of a high-voltage plasma discharge in the system while trying to evaporate high-T_c superconductor powders. Inficon rate monitor units and systems, along with control systems, were troubleshot and repaired for the same reason. SFA replaced the poppet assembly in the E-beam.

SFA personnel also built equipment to supplement existing equipment or automate manual processes. SFA automated the controlled opening and closing of an E-beam source for the evaporation and deposition of alloy, bilayer, and multilayer thin films by interfacing the stepper-motor's controller with a computer. This interface integrated the system and placed the computer in control of the stepper-motor's timing, speed, direction, and position. SFA also designed and fabricated the following devices: a non-inductive heater unit for in situ annealing of magnetic materials in a magnetic field, a shutter macrocosm for the deposition of alloys and multilayers in the E-beam, and a tunable filter for material characterization.

Superconducting Measurements

SFA personnel measured the temperature dependence of the magnetic susceptibility of potential superconducting or magnetic samples, making use of the Materials Physics Branch's SQUID magnetometer system. Specifically, SFA personnel measured and analyzed the magnetic properties of high-temperature superconductors and made magnetic and electrical measurements of high-T_c materials. To determine the critical temperature of a material, SFA measured its change in resistance, magnetic permeability, and heat capacity. The magnetic method is a probeless technique that depends on a large decrease in magnetic permeability as the material goes superconducting. The advantages of using this method are that it requires no direct electrical contacts with the sample, is non-destructive, and may be used with samples that are small, irregular, or in powder form. The magnetic measurements on high-temperature superconductors were performed for the following purposes:

- To screen and test for new superconducting materials;
- To study and analyze the properties of known superconductors;
- To study the various phases of high-temperature superconductors;
- To improve magnetic measuring methods and techniques;
- To determine the best way to measure and define the critical temperature of these multi-phased materials; and
- To establish standard techniques and materials to use as a temperature reference.

SFA personnel studied various properties of new high-temperature superconducting materials and analyzed the behavior of layered high case temperature oxides in an external field. This analysis was directly related to developing a capability for making such new devices as microwave cavities and infrared bolometers. SFA personnel studied the response, surface resistance, and impact of the multi-gap structure on the temperature dependence of the parameters. The renormalizations of different quantities, such as magnetic susceptibility, Sommerfield's constant, and effective mass, were also studied. This study produced important information about the relaxation phenomena and interaction of the carriers with different collective modes. SFA was par-

ticularly concerned with analyzing the behavior of electronic heat capacity in the high-temperature region, as well as such transport phenomena as thermal conductivity and thermopower.

SFA personnel studied alloy thin films, specifically iron in ruthenium and cobalt in copper. The samples were annealed at different temperatures. SFA studied the composition and structure of the films using X-ray methods, and the magnetic and electrical effects using resistivity and magnetoresistance measurements at low temperatures. The study of the iron-ruthenium system showed that the iron alloyed with the ruthenium but did not phase separate, even at higher temperatures. The studies of cobalt in copper showed a phase separation at 300°C with enhanced grain growth at higher temperatures. The cobalt in copper system demonstrated the desired effect.

SFA personnel specifically studied thallium-strontium-calcium-copper-oxygen, thallium-barium-calcium-copper-oxygen, lanthanum-doped thallium, yttrium-doped thallium, and cobalt systems. Standard ceramic processing techniques were used for all systems except thallium. Because of its toxicity, the methods used for working with thallium systems required special safety equipment encasement in gold tubing during the reaction. This work achieved a higher case temperature material for use in lossless transmission lines and other electronic devices.

SFA personnel also conducted environmental effects studies on new superconducting materials. For instance, thermal cycling was performed on the test subjects by dipping them in liquid nitrogen, thus demonstrating the survivability of films in space applications.

APPENDIX

Table of Contents

Structural and magnetic properties of ion beam sputtered deposited Cu/Fe multilayers

(Received 9 October 1990; accepted 22 October 1990)

Fe/Cu multilayers have been deposited using the ion assisted/ion beam sputtering technique. X-ray diffraction and selected area transmission electron diffraction show that Fe is in the body-centered-cobic phase. These results were in agreement with extended x-ray absorption fine structure measured at the Fe *K* edge using synchrotron radiation. Magnetic measurements using vibrating sample magnetometer and ferromagnetic resonance show nominal moment of the Fe, but moderate out of plane anisotropy.

I. INTRODUCTION

Compositionally modulated multilayered films (CMF) involving ferromagnetic layers separated by nonmagnetic interlayers have attracted great interest because of their unusual magnetic and structural properties.[1-4] Recently Heinrich *et al.* reported a new phase of Cu for ultrathin Fe/Cu/Fe trilayers grown by molecular-beam epitaxy on Ag(001) substrates.[5] Previous studies reported the formation of face-centered-cubic (fcc) Fe when grown on Cu(100).[6,7] Although there are also reports on the structural and magnetic properties of Cu/Fe CMF, the structure and magnetic properties have not been clarified yet.[8,9] In this paper we have investigated the structural and magnetic properties of Cu/Fe multilayers grown by the ion beam assisted deposition (IBAD) technique. X-ray diffraction (XRD) and extended x-ray absorption fine structure (EXAFS) techniques were used to obtain structure of the Fe layers in Cu/Fe multilayers and these results were confirmed by transmission electron diffraction. Magnetic properties of samples grown with and without ion-beam assist have been compared.

II. EXPERIMENTAL DETAILS

The compositionally modulated Cu/Fe thin films were deposited on Si and glass substrates in a computer controlled dual ion beam sputtering system. The base pressure was typically 1.5×10^{-7} Torr in the sample chamber prior to deposition. Argon beams were injected into the system from two 3.0 cm Kaufman ion sources. The details of deposition are described elsewhere.[10] X-ray diffraction scans were obtained using a rotating anode with a Cu target. Selected area transmission electron diffraction patterns were obtained from cross-sectional specimens using 200 kV electrons. X-ray absorption fine structures (XAFS) were measured at the *K* edge of Fe using conversion electron detection to determine the structure of Fe film in Cu/Fe multilayer.[11] The magnetic properties of the samples were measured using vibrating sample magnetometer (VSM) and ferromagnetic resonance (FMR).

III. RESULTS AND DISCUSSION

A. Structural characterization

Figure 1 shows a low angle x-ray diffraction pattern of Cu/Fe CMF (designated as 82-1) taken with Cu $K\alpha$ radiation on Rigaku rotating anode machine. Three diffraction peaks corresponding to the periodic structure of the Cu/Fe CMF can be seen. However the high angle diffraction pattern of Cu/Fe which is shown in Fig. 2 shows no satellite peaks. This could be attributed to poor crystallinity and small crystallite size and the spread of the crystallographic orientation.

Although XRD (Fig. 2) shows only one diffraction with a *d* spacing equal to that Cu(111), annealing the sample in vacuum up to 500 °C showed both the Cu(111) and Fe(110) peaks. Figure 2 shows the diffraction pattern of Fe/Cu CMF(82-1) as a function of annealing temperature. It took about 1/2 h to stabilize the temperature and 1/2 h to obtain diffraction scan. From this figure it is clear that Fe film of the multilayer undergoes crystallization when annealed up to 500 °C for periods of the order of few hours. The wavelength of CMF was obtained from low angle-diffraction peaks after carrying out the correction of refractive index of Cu/Fe for

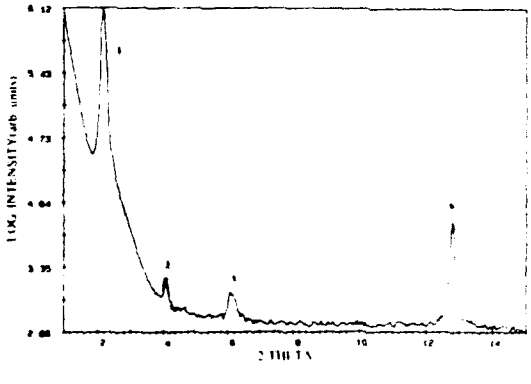

FIG. 1. X-ray low angle 2θ diffraction pattern of Fe (16.5 Å) and Cu (21.5 Å) [sample 82-1], CMF using Cu $K\alpha$ radiation.

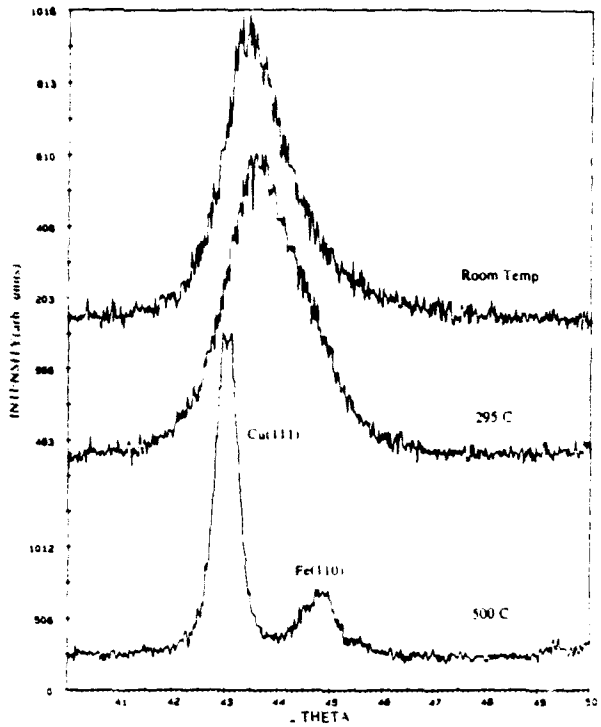

FIG. 2. 2θ—x-ray diffraction scan of Cu(111)/Fe(110) multilayer taken at room temperature and at elevated temperatures. [sample 82-1]

Cu $K\alpha$ radiation. The wavelength of the CMF thus obtained was within 5% agreement from the value obtained from x-ray fluorescence (XRF) measurements as shown in Table I. In XRF measurements the total thicknesses of Fe and Cu were estimated by comparing the signals of characteristic lines from Fe and Cu with their corresponding standards of known thicknesses. Once the total thickness of each component was obtained then the CMF wavelength is calculated by dividing the sum of thicknesses of the components by the number of layers. Selected area electron diffraction showed the films to be mixtures of body-centered-cubic (bcc) Fe and fcc Cu. From Fig. 3 it is clear that the multilayers exhibit $Cu(111)_{fcc}/Fe(110)_{bcc}$ fiber texture.

In order to ascertain the structure of Fe, x-ray absorption fine structure (XAFS) of these samples were measured at the K edge of Fe using conversion electron detection at the National Synchrotron Light Source.[11] An Fe film alone was also measured by the same method for comparison. The raw data were normalized by the edge step after a linear pre-edge background substraction. The normalized spectra of Fe/Cu (82-1 and 87-1) samples and the Fe film are shown in Fig. 4. We can see from the figure that the spectra of Cu/Fe samples are similar to that of Fe film, with reduced amplitudes. Further analysis was done following the standard EXAFS analysis procedure.[12] Fourier transforms obtained show peaks characteristic of bcc structure.

B. Magnetic properties of Cu/Fe multilayer films

The magnetic properties of the multilayer Cu/Fe films were measured using VSM and FMR. All measurements were made at room temperature. In general, the films were magnetically soft with coercivities of about 1 Oe for fields in the film plane, and FMR linewidths of about 30 Oe at 8 GHz. However, the properties do differ considerably from

TABLE I. Magnetic properties of Cu/Fe multilayers of sample 82-1 (ion assisted) and sample 87-1 (nonassisted).

Sample		82-1 (ion assisted)	87-1 (no assist)
Perpendicular *BH* curve		Very small curvature	Considerable curvature
Second phase amount		3% of moment	10% of moment
Total $4\pi M$/Fe volume		17.50 kG	18.90 kG
Knee field		11.50 kG	11.80 kG
Effective $4\pi M$ from FMR		11.72 kG	12.35 kG
FMR linewidth at	4 GHz	35 Oe	19 Oe
	8 GHz	45 Oe	29 Oe
	35 GHz	200 Oe	160 Oe
CMF period λ by XRF		37.8 A	32.5 A
CMF period λ by XRD		38.0 A	34.0 A

FIG. 3. Electron diffraction of Cu/Fe [sample 82-1] multilayer. 1, 2 are Cu(111) and (200) diffraction rings, 3 corresponds to Fe(200) while the Fe(110) ring overlaps with Cu(111).

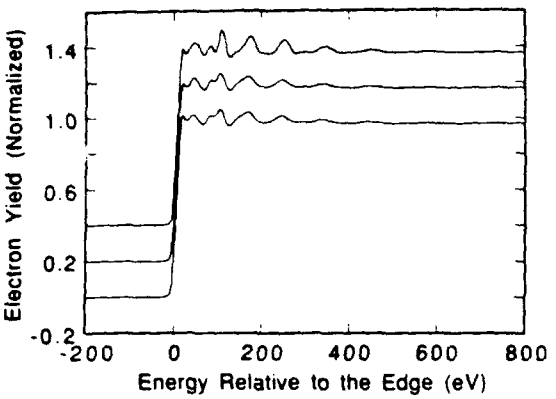

FIG. 4. Normalized XAFS of Fe K-edge spectra for Fe film (top), Cu/Fe [sample 82-1] (middle) and Cu/Fe [sample 87-1] (bottom). Top two spectra are shifted vertically for clarity.

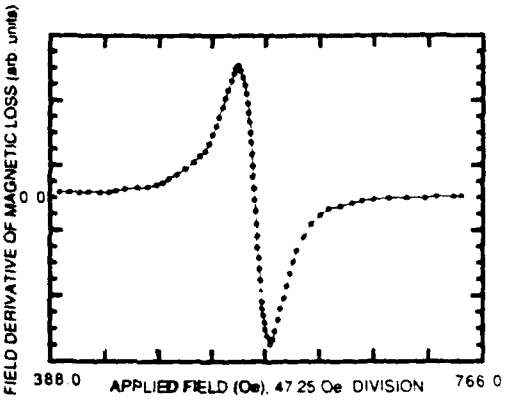

FIG. 6. 8 GHz FMR data taken with the applied field H in the film plane. The ordinate is proportional to the field derivative of the magnetic loss.

those of bulk iron in several ways: the magnetic moments are slightly reduced, there is considerable anisotropy favoring the out-of-plane orientation, and there is evidence of a small fraction of the iron being magnetically isolated from the bulk.

The M–H curves for the sample 87-1 are shown in Fig. 5 for fields applied both in the film plane and perpendicular to it. Figure 6 shows the FMR signal taken at 8 GHz (field derivative of magnetic losses) for the sample prepared without ion assist.

The properties of the two samples are summarized in the Table I. The total $4\pi M$ was determined by dividing the total moment as found by VSM by a volume corresponding to the total amount of iron in the sample. Some reduction of M relative to the 21 kG value of bulk iron is expected because of the reduced dimensionality of these films; any iron in an amorphous or fcc state could have a much reduced moment; finally, Fe isolated as very small particles would be paramagnetic and not easily seen in our measurements. Some evidence of this was seen in the sample prepared without ion assist: the FMR showed a broad signal corresponding to a system with g of about 2 and no significant net moment or anisotropy.

Perpendicular field M–H loops similar to those shown in Fig. 5 above have been reported in Cu/Ni multilayer films. Atzmony *et al.*[13] reported time dependent effects suggestive of superparamagnetism in such films.

Both of our films show moderately lower effective magnetization as determined by FMR and location of the M–H curve knee than found from the total moment. Evidently, in addition to demangnetization, another mechanism is present which favors the in-plane orientation of the moment (different directions in the plane differ only slightly). Such effects have been previously reported[5] for very thin iron layers and are attributed to an anisotropy on the order of an erg/cm^2 acting on the surface layer.

In summary, Cu/Fe multilayers appear to be another example[14] of very soft magnetic systems which can be produced when Fe grain size is restricted by the requirement to renucleate on a scale small compared to typical magnetic relaxation lengths. A large anisotropy favoring the out-of-plane orientation apparently arises at the Cu/Fe interfaces.

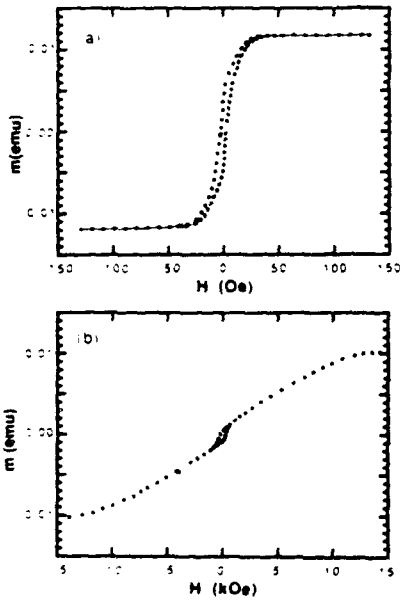

FIG. 5. M–H data taken using VSM for sample 82-1 with (a) applied field in the film plane and (b) applied field perpendicular to the film plane.

IV. CONCLUSIONS

Cu/Fe CMFs grown by dual ion beam sputtering show that Fe layers are in the bcc phase as determined by XRD, electron diffraction, and EXAFS measurements. The moment of Fe is slightly lower than that of bulk iron, and may be attributed to reduced dimensionality.

ACKNOWLEDGMENT

One of the authors (K.H.K.) acknowledges support by the National Research Council. Part of the research was car-

ried out at the National Synchrotron Light Source, Brookhaven National Laboratory, which is supported by the U.S. Department of Energy, Division of Materials Sciences and Division of Chemical Sciences.

[1] T. Shingo, N. Hosoito, K. Kawaguchi, T. Takada, Y. Endoh, Y. Ajiro, and M. Friedt, J. Phys. Soc. Jpn. **52**, 3154 (1983).
[2] Y. Kozono, M. Komuro, S. Narishige, M. Hanazono, and Y. Sugita, J. Appl. Phys. **61**, 4311 (1987).
[3] Z. S. Shan, Z. R. Zhao, J. G. Zhao, and D. J. Sellmyer, J. Appl. Phys. **61**, 4320 (1987).
[4] M. Nagkubo, T. Yamamoto, and M. Naoe, J. Appl. Phys. **64**, 5751 (1988).
[5] B. Heinrich, Z. Celinski, J. F. Cochran, W. B. Muir, J. Rudd, Q. M. Zhong, A. S. Arrott, K. Myrtle, and J. Kirschner, Phys. Rev. Lett. **64**, 673 (1990).
[6] D. A. Steigerwald and W. F. Egelhoff, Jr., Surf. Sci. **192**, L877 (1987).
[7] W. A. Jesser and J. W. Matthews, Philos. Mag. **15**, 1097 (1967).
[8] H. J. G. Draaisma, H. M. Van Noort, and F. J. A. Den Broeder, Thin Solid Films **126**, 117 (1985).
[9] T. Katayama, H. Awano, and Y. Nishihara, J. Phys. Soc. Jpn. **55**, 2539 (1986).
[10] C. Kim, S. B. Qadri, H. Y. Yu, K. H. Kim, B. Maruyama, and A. S. Edelstein, J. Vac. Sci. Technol. A **8**, 11407 (1990).
[11] W. T. Elam, J. P. Kirkland, R. A. Neiser, and P. D. Wolf, Phys. Rev. B **38**, 26 (1988).
[12] D. E. Sayers, and B. A. Bunker in *X-ray Absorption*, edited by D. C. Koningsberger and R. Prins (Wiley, New York, 1988).
[13] U. Atzmony, L. J. Swartzendruber, L. H. Bennett, M. P. Dariel, D. Lashmore, M. Rubinstein, and P. Lubitz, J. Magn. Magn. Mat. **69**, 237 (1987).
[14] T. Kobayashi, R. Naketani, S. Otomo, and N. Kumasaka, IEEE Trans. Magn. MAG **23**, 2748 (1988); M. Senda and Y. Nagai, J. Appl. Phys. **65**, 1238 (1989).

Ion-beam deposition of Ag/Fe multilayers and their structural and magnetic properties

Ag/Fe multilayers of Ag and Fe have been synthesized using ion assisted ion-beam deposition technique. Low angle peaks and well-defined satellite peaks at high angle were recorded indicating the periodic structure and the sharpness of the interface. Read photograph and selected area electron diffraction show that Fe is in bcc structure in Ag/Fe multilayers. Magnetic moment of the Ag/Fe film is comparable to bcc Fe.

I. INTRODUCTION

Multilayers involving ferromagnetic layers and nonmagnetic layers have attracted great attention because of their unusual magnetic and structural properties.[1-4] Superlattices of Ag/Fe have been grown by a variety of techniques,[5-8] such as molecular beam epitaxy, sputtering, etc., and their structural and magnetic properties have been studied. Sharp interfaces of Ag/Fe multilayers were obtained and they could be attributed to the fact that Ag does not alloy with other transition metals. Krishnan and Tessier[9] reported that samples prepared by rf sputtering under certain conditions of preparation exhibit high magnetization and Faraday rotation. Several magnetic studies of Ag/Fe have been carried out using ferromagnetic resonance (FMR),[10] conversion-electron Mossbauer,[8] and spin polarized photoemission.[7]

In the present paper we describe the deposition of Ag/Fe multilayer films using dual ion beam sputtering technique and study their structural and magnetic properties.

II. EXPERIMENTAL

The multilayers of Ag/Fe were deposited on Si(001) and glass substrates using sputtering in a computer controlled dual-ion-beam system. The base pressure was typically 1.5×10^{-7} Torr prior to deposition. One argon beam was directed toward the target material and the other toward substrate. The details of deposition are described elsewhere.[11] X-ray diffraction scans were obtained on a conventional diffractometer with a rotating anode using Cu$K\alpha$ radiation. The magnetic properties of the samples were measured using vibrating sample magnetometer (VSM) and ferromagnetic resonance (FMR).

III. RESULT AND DISCUSSION

A. Structural characterization

Figure 1 shows a low angle x-ray diffraction from Ag–Fe multilayer (82-1) taken with Cu$K\alpha$ radiation. The period obtained from the diffraction peak is in very good agreement with the period obtained through energy dispersive x-ray fluorescence analysis. Figure 2 shows the diffraction scan at high angle near Ag(111) and bcc Fe(110) or fcc Fe(111) diffraction peaks. Well-defined satellite peaks can be seen around Ag(111), showing the periodic structure of Ag/Fe layers. The period obtained from the satellite peaks was essentially the same as obtained from the low angle diffraction peak.

The Fe peak is broad and the corresponding satellite peaks are not observed. The criteria for resolution, as given in our previous work,[12] is satisfied if one takes into consideration the d spacings of Ag(111) and Fe(110) bcc or Fe(111) fcc. The lattice parameter obtained from Ag(111) is in agreement with the bulk value for Ag. If it is assumed that the d spacings of the broad peak corresponds to bcc Fe(110), then one obtains a lattice parameter of 2.94 Å. On the other hand, if one assumes the d spacings correspond to Fe(111) fcc phase then one obtains for Fe lattice parameter of 3.59 Å, which is in good agreement with the value expected for fcc Fe lattice parameter. However, a full scan ranging from 20 to 120 showed other peaks of Fe, which were indexable as (200) and (211), based on a lattice parameter of 2.94 Å for bcc Fe. Read photographs taken with Fe$K\alpha$ radiation showed the presence of fcc phase of Ag only and no diffraction lines from bcc Fe were seen (Fig. 3). Selected area electron diffraction showed rings corresponding to fcc Ag and spots that were indexable based on Fe bcc with a lattice parameter of 2.94 Å. Two films designated 83-1 and 84-1 have been the focus of study in the present investigation. For 84-1 individual Fe layer thickness was 15.2 Å and Ag layer thick-

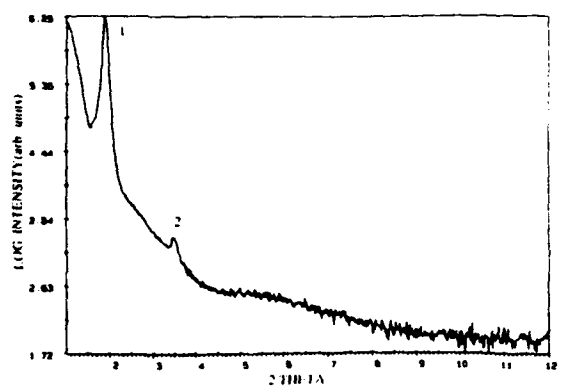

FIG. 1. X-ray low angle 2θ diffraction pattern for Ag(30 Å)–Fe(16 Å) (sample 83-1) multilayer using Cu$K\alpha$ radiation.

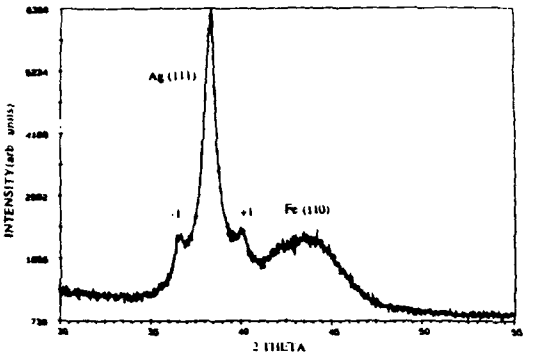

FIG. 2. The 2θ x-ray diffraction of Ag/Fe (sample 83-1) multilayer taken with Cu$K\alpha$ radiation.

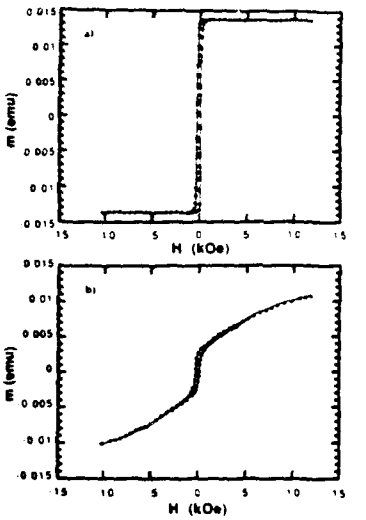

FIG. 4. The M–H data taken VSM for sample 84-1 with (a) the applied field in the film plane and (b) the applied field perpendicular to the film plane

ness 21.2 Å, whereas for 83-1 Ag thickness was around 30 Å. These two films showed similar structural characteristics.

B. Magnetic properties of Ag/Fe multilayer films

The magnetic properties of the multilayer Ag/Fe films were measured using VSM and FMR. All measurements were made at room temperature.

The film 83-1 was magnetically soft with coercivity of a few Oersteds for fields in the film plane, and FMR line widths of about 33 Oe at 8 GHz. The in-plane magnetic moment was comparable with that of bulk iron. However, the FMR indicates that there is an anisotropy favoring the out-of-plane orientation, thereby reducing the effective $4\pi M$, as deduced from the resonance field or the knee of the M–H curve by about 8 kOe. Similar effects, attributed to a surface anisotropy, have been reported for thin Fe layers with Ag surfaces.[13]

The film 84-1 has properties qualitatively similar to 83-1,

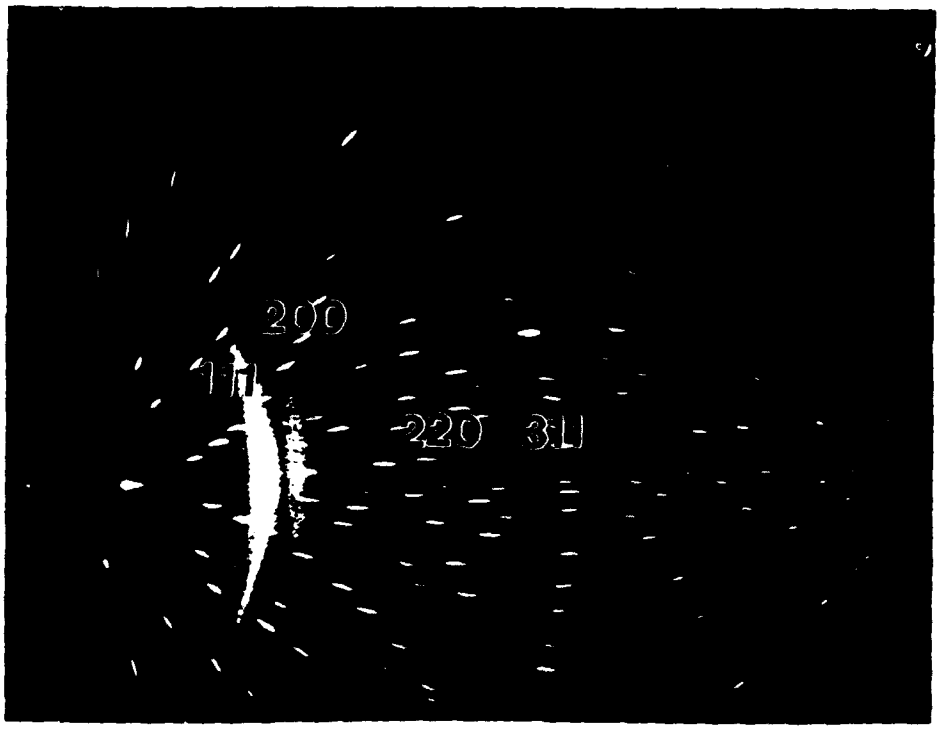

FIG. 3. Read photograph of Ag/Fe (sample 83-1) multilayer taken with Fe$K\alpha$ radiation.

although the line width was about 50% higher, and the in-plane anisotropy field and the coercive field were slightly larger.

Using VSM (see Fig. 4), we observe for sample 84-1 a somewhat rounded M–H curve in the perpendicular orientation and a component comprising about one-third of the total moment, which saturates at very low fields. Sample 83-1 shows a similar but smaller effect. This component appears to be a separate system, which does not experience the overall demagnetization effects. It may represent a part of the sample for which the local perpendicular anisotropy exceeds the local demagnetizing field. Such M–H curves have been reported in Cu/Ni multilayer films. Atzmony *et al.*[14] reported time-dependent effects suggestive of superparamagnetism in such films.

IV. CONCLUSION

X-ray diffraction, selected area electron diffraction shows that Fe is in bcc phase in Ag/Fe multilayers grown by the dual-ion-beam deposition technique. The magnetic properties of Ag/Fe are comparable to that of bulk bcc Fe.

[1] T. Shingo, N. Hosoito, K. Kawaguchi, T. Takada, Y. Endoh, Y. Ajiro, and M. Friedt, J. Phys. Soc. Jpn. **52**, 3154 (1983).
[2] Y. Kozono, M. Komuro, S. Narishige, M. Hanazono, and Y. Sugita, J. Appl. Phys. **61**, 4311 (1987).
[3] Z. S. Shan, Z. R. Zhao, J. G. Zhao, and D. J. Sellmyer, J. Appl. Phys. **61**, 4320 (1987).
[4] M. Nagakubo, T. Yamamoto, and M. Naoe, J. Appl. Phys., **64** (10), 5751 (1988).
[5] Y. Kozono, M. Komuro, S. Narishige, M. Hanazono, and Y. Sugita, J. Appl. Phys. **63**, 3470 (1988).
[6] J. Q. Xiao, A. Gavrin, Gang Xiao, W. A. Bryden, C. L. Chien, and A. S. Edelstein, J. Appl. Phys. **67**, 5388 (1990).
[7] B. T. Jonker, K. H. Walker, E. Kisker, G. A. Prinz, and C. Carbone, Phys. Rev. Lett. **57**, 142 (1986).
[8] N. C. Koon, B. T. Jonker, F. A. Volkening, J. J. Krebs, and G. A. Prinz, Phys. Rev. Lett. **59**, 2463 (1987).
[9] R. Krishnan and M. Tessier, J. Appl. Phys. **67**, 5391 (1990).
[10] B. Heinrich, K. B. Urquhart, A. S. Arrott, J. F. Cochran, K. Myrtle, and S. T. Purcell, Phys. Rev. Lett. **59**, 1756 (1987); B. Heinrich, K. B. Urquhart, J. R. Dutcher, S. T. Purcell, J. F. Cochran, A. S. Arrott, D. A. Steigerwald, and W. F. Egelhoff, Jr., J. Appl. Phys. **63**, 3863 (1988).
[11] C. Kim, S. B. Qadri, H. Y. Yu, K. H. Kim, B. Maruyama, and A. S. Edelstein, J. Vac. Sci. Technol. A **8** (3), 1407 (1990).
[12] C. Kim, S. B. Qadri, M. Twigg, and A. S. Edelstein, J. Vac. Sci. Technol. A **8**, 3466 (1990).
[13] J. J. Krebs, B. T. Jonker, and G. A. Prinz, J. Appl. Phys. **63**, 3467 (1988).
[14] U. Atzmony, L. J. Swartzendruber, L. H. Bennett, M. P. Dariel, D. Lashmore, M. Rubinstein, and P. Lubitz, J. Magn. and Magn. Mater. **69**, 237 (1987).

Low-field spin-valve magnetoresistance in Fe-Cu-Co sandwiches

A. Chaiken,[a] P. Lubitz, J. J. Krebs, G. A. Prinz, and M. Z. Harford
Naval Research Laboratory, Code 6345, Washington, DC 20375

(Received 11 March 1991; accepted for publication 1 May 1991)

Fe-Cu-Co sandwiches have been grown on glass and silicon substrates using electron beam evaporation. Because the typical coercive field of a thin Co film is higher than that of a typical Fe film, the magnetization curves of these sandwiches show clearly the separate, sequential reversal of the Fe and Co moments as a function of applied field. In the applied field region where the moments of the two magnetic layers are antialigned, the spin-valve magnetoresistance shows a peak of over 3% in amplitude at room temperature.

Both exchange-coupled[1] and uncoupled[2,3] ferromagnet-paramagnet-ferromagnet sandwiches and superlattices display a large negative magnetoresistance (MR) when the moments of adjacent ferromagnetic layers are turned from antiparallel to parallel. The isotropic positive magnetoresistance associated with the antiparallel alignment has been called the spin-valve effect.[3] In superlattices which have an antiferromagnetic interlayer exchange, the antialigned state occurs at zero applied field,[1,4] and is the ground state of the system. In the uncoupled sandwiches, the antialignment occurs for a finite range of applied fields, and is possible either because of an exchange bias pinning of one of the ferromagnetic moments,[3] or because of different coercivities in thick and thin Co layers.[2]

Another method of obtaining different coercive fields in alternate layers of a superlattice is to make those layers of different ferromagnetic metals. Shinjo and Yamamoto have reported results on Co-Cu-NiFe superlattices.[5] The Fe-Cu-Co system is another good choice because of the limited miscibility of the Fe and Co in Cu at low fabrication temperatures, and because the growth of these metals is already well understood.[6] For the present study, polycrystalline Fe, Cu, and Co layers were sequentially electron beam evaporated from elemental sources onto untreated glass or silicon (100) substrates. Layer thicknesses were monitored during deposition with a quartz crystal oscillator, and checked via x-ray fluorescence measurements. The background pressure of the vacuum system is about 10^{-7} torr.

Figure 1(a) shows magnetization curves for two Fe-Cu-Co sandwiches grown during the same run, but deposited at different substrate temperatures of 220 and 165 °C. As the figure illustrates, sandwiches grown at temperatures 220 °C and above reproducibly have square magnetization curves, indicating that the Fe and Co moments are reversing together. However, in the sandwiches deposited at 165 °C and below, the Co and Fe do indeed have different coercivities, as demonstrated by the presence of the shoulder in the magnetization curve at $H \approx 0.1$ kOe. For the increasing field part of the loop, the shoulder corresponds to the field region where the moment of the Fe film has already reversed, but the moment of the Co film is just beginning to rotate. The identification of the higher coercivity part of the loop with the Co film has been confirmed by a study on a series of samples with different Co thicknesses. Similar magnetization curves were reported in Ref. 5 for NiFe-Cu-Co superlattices. The disappearance of the shoulder in the magnetization curve between 165 and 220 °C is attributed to slight interdiffusion of the Cu and

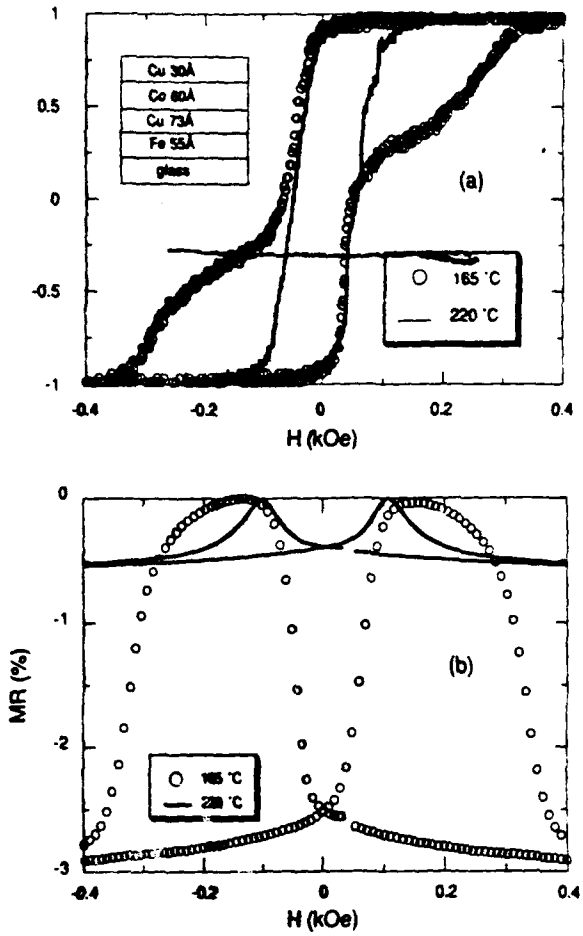

FIG. 1. (a) Magnetization curves for two Fe-Cu-Co-Cu sandwiches (see inset) grown on glass at different deposition temperatures. The shoulder in the magnetization of the 165 °C sample indicates the region where the Fe and Co moments are antialigned. (b) Room-temperature transverse magnetoresistance curves for the same two samples. The 220 °C sample with the square magnetization curve has an MR trace typical for a single, thin ferromagnetic film, whereas the 165 °C sample has an increased resistance when the moments of the two films are antialigned.

[a]NRL postdoctoral associate.

 0003-6951/91/270240-03$02.00

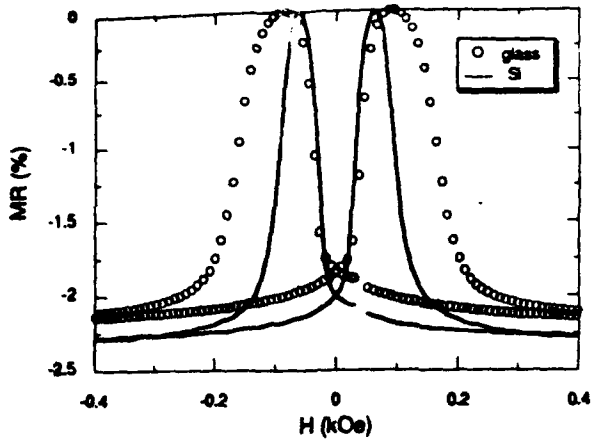

FIG. 2. Transverse magnetoresistance for two Fe51 Å/Cu55 Å/Co48 Å sandwiches which were deposited simultaneously, one on glass and one on a semi-insulating Si substrate. The growth temperature was 165 °C.

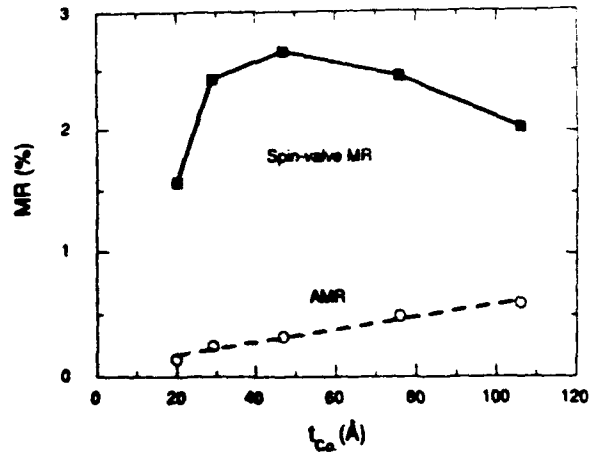

FIG. 3. Co thickness dependence of the anisotropic magnetoresistance (AMR) and spin-valve magnetoresistance for a series of Fe-Cu-Co-Cu sandwiches. These samples were deposited on glass at 165 °C, and had the structure Fe56 Å/Cu50 Å/Co(t_{Co})/Cu30 Å.

ferromagnetic layers. Recent Auger electron spectroscopy and thermal energy atom scattering studies of the Co/Cu system by de Miguel *et al.*[6] show that diffusion of Cu into Co begins at about 177 °C. No significant in-plane magnetic anisotropy is observed in the magnetization curves of these two samples despite the presence of bias fields up to 50 Oe during deposition.

Figure 1(b) shows magnetoresistance data for the same two sandwiches at room temperature. The magnetoresistance is here defined to be the ratio of the field-induced change in resistance to the zero-field resistance. The 220 °C sample has an MR curve that is typical for thin ferromagnetic films, with a peak of 0.5% near the coercive field of the magnetization curve. For the 165 °C sandwich, the peaks in the magnetoresistance correspond well to the region of the magnetization curve where the Fe and Co moments are maximally antialigned, as expected. The magnitude of the transverse MR at magnetic saturation is 3.1% for this sandwich, comparable to the room-temperature MR previously found for uncoupled sandwiches.[2,3] The anisotropic magnetoresistance (AMR) for the 165 °C sample was measured directly at 3 kOe to be 0.41%. The spin-valve component of the magnetoresistance is the transverse MR (applied field perpendicular to the current direction) minus half the AMR.[7] Therefore the component of the MR attributable to the spin-valve effect is 2.9%. A spin-valve magnetoresistance of over 3% at room temperature can be obtained even in simple Fe-Cu-Co sandwiches by optimizing the deposition temperature and the layer thicknesses.

Figure 2 shows magnetoresistance data for two Fe51 Å/Cu55 Å/Co48 Å sandwiches grown simultaneously at 165 °C, one on glass and one on Si. The Fe films of both samples switch between 0 and about 0.05 kOe. However, the Co moment in the sample grown on glass reverses at a significantly higher field than the Co moment in the Si sample, as demonstrated by the corresponding M–H loops (not shown). This variability in the behavior of the Co layer is somewhat surprising given that it is the Fe layer which is deposited directly on the substrate. The deposition temperature variation in Fig. 1 also principally affects the behavior of the Co layer. X-ray diffraction and cross-sectional transmission electron microscopy studies are currently underway to look for associated structural changes in the Co film or the interface quality.[8]

In order to make a comparison to the previous transport studies on both coupled and uncoupled sandwiches, it is interesting to examine the dependence of the spin-valve MR on individual layer thickness. Figure 3 shows the variation of the AMR and spin-valve MR with Co thickness. The linear thickness dependence of the AMR is expected and is due simply to the increase of the amount of ferromagnetic material in the sample. On the other hand, the nonmonotonic form of the spin-valve magnetoresistance cannot be simply explained. The broad peak is similar to that observed by Dieny *et al.* in their exchange-biased sandwiches.[3] Further investigation of this thickness dependence is under way, as is a detailed study of the variation of the spin-valve effect with Cu and Fe thickness.

In conclusion, the spin-valve magnetoresistance has been observed in a new sandwich system, Fe-Cu-Co. The large ($>3\%$) MR reproducibly achievable in polycrystalline films on silicon and glass at applied fields of only 1 00 Oe may have technological significance. The spin-valve magnetoresistance and its associated magnetization curve are suppressed by interlayer interdiffusion, as indicated by a growth temperature study. The variation of the spin-valve MR with Co thickness may be a clue to its fundamental origin.

We thank D. King for the x-ray measurements. This research was supported by DARPA and ONR.

[1] M. N. Baibich, J. M. Broto, A. Fert, F. Nguyen van Dau, F. Petroff, P. Etienne, G. Creuzet, A. Friederich, and J. Chazelas, Phys. Rev. Lett. 61, 2472 (1988).
[2] C. Dupas, P. Beauvillain, C. Chappert, J. P. Renard, F. Trigui, P. Veillet, E. Vélu, and D. Renard, J. Appl. Phys. 67, 5680 (1990).

[3]B. Dieny, V. S. Speriosu, S. S. P. Parkin, B. A. Gurney, D. R. Wilhoit, and D. Mauri, Phys. Rev. B 43, 1297 (1991).
[4]P. Grunberg, R. Schreiber, Y. Pang, U. Walz, M. B. Brodsky and H. Sowers, J. Appl. Phys. 61, 3750 (1987).
[5]T. Shinjo and H. Yamamoto, J. Phys. Soc. Jpn. 59, 3061 (1990).
[6]J. J. de Miguel, A. Cebollada, J. M. Gallego, R. Miranda, C. M. Schneider, P. Schuster, and J. Kirschner, J. Magn. Magn. Mater 93, 1 (1991), and references therein.
[7]A. Chaiken, G. A. Prinz, and J. J. Krebs, J. Appl. Phys. 67, 4892 (1990).
[8]J. Kim and L. Salamanca Riba (unpublished)

Surface and Coatings Technology, 49 (1991) 139-142

Structural and magnetic properties of Al/Fe multilayers deposited by ion beam sputtering

S. B. Qadri, C. Kim, M. Twigg, M. Z. Harford* and P. Lubitz
U.S. Naval Research Laboratory, Washington, DC 20375 (U.S.A.)

Abstract

Al/Fe multilayers were deposited using an ion-assisted ion-beam sputtering technique. X-ray diffraction at high angles showed peaks corresponding to the aluminum f.c.c. phase with a lattice parameter equal to that of bulk aluminum. Peaks from the iron b.c.c. phase were observed and the lattice parameter based on these peaks was calculated to be 2.94 Å. The absence of satellite peaks is attributed to the small grain size. The low angle diffraction pattern showed three orders of peaks. Investigation of the magnetic properties using a vibrating sample magnetometer and ferromagnetic resonance showed a moderately reduced moment for iron when compared with bulk iron.

1. Introduction

Multilayered films of ferromagnetic layers separated by non-magnetic layers have attracted considerable attention because of their interesting magnetic and structural properties [1-4]. Recent reports [5, 6] indicated the formation of f.c.c. iron when grown on Cu(100) and a new phase of copper for Fe/Cu/Fe trilayers grown by molecular beam epitaxy on Ag(001) substrates. More recently we investigated the structural and magnetic properties of Cu/Fe, Ag/Fe and Fe/Ni grown by ion-beam assisted deposition (IBAD) and found the formation of f.c.c. iron in Fe/Ni for a certain range of wavelengths [7-9]. Fe/Al multilayers were deposited by Nagakubo *et al.* [4] using ion beam sputtering and the relationship between the crystal structure and magnetic properties was discussed. In this paper we report the results on Fe/Al layers deposited by a dual-ion-beam technique, with ion beam assistance and without ion beam assistance during the deposition process, and compare their magnetic and structural properties.

2. Experimental details

The multilayers of Al/Fe were deposited onto silicon and Corning glass substrates in a computer-controlled dual-ion-beam sputtering system. The base pressure of the sample chamber was of the order of 1.5×10^{-7} Torr prior to deposition. Argon beams were injected into the system from two 3.0 cm Kaufman ion guns. The complete details of the deposition are described elsewhere [9]. X-ray diffraction scans were obtained using a Rigaku diffractometer and a rotating anode X-ray generator with a copper target. Selected area electron diffraction and cross-sectional transmission electron microscopy (XTEM) were also used to study the structure of these multilayers. The magnetic properties of the samples were measured using a vibrating sample magnetometer (VSM) and ferromagnetic resonance (FMR).

3. Results and discussion

3.1. Structural characterization

Figure 1 shows a small angle X-ray diffraction pattern of Al/Fe for a non-assisted sample taken with Cu $K\alpha$ radiation. Three distinct orders of peaks corresponding to the superlattice structure of Al/Fe multilayers can be seen. The wavelength computed using these three peaks was in good agreement when compared with the value obtained from X-ray fluorescence measurements and from the deposition rate. Figure 2 shows the diffraction scan taken for 2θ values between 20° and 100°. Peaks corresponding to b.c.c. iron are indexed along with peaks for f.c.c. aluminum. The absence of satellite peaks is attributed to the small grain size. The lattice parameter of iron calculated based on the observed peaks is 2.94 Å and is enhanced in comparison with the bulk value of 2.866 Å. This enhancement for the b.c.c. iron film was also observed in our earlier measurements on the Ag/Fe system [8]. The iron layers exhibited (110) preferred orientation for a layer thickness of 13 Å. This result is in contrast to that of

*Sachs Freeman Associates, Inc., Landover, MD 20785, U.S.A.

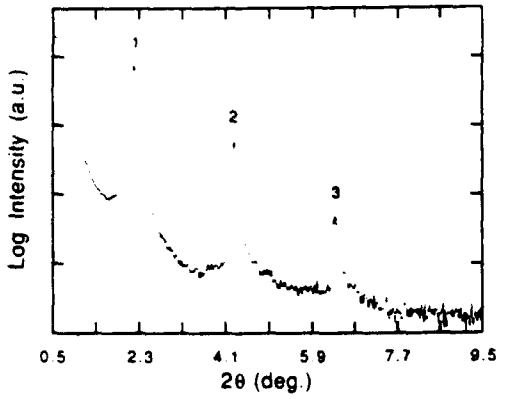

Fig. 1. X-ray low angle 2θ diffraction pattern taken using Cu Kα radiation of an Al(29 Å)/Fe(13 Å) multilayer deposited without ion beam assistance.

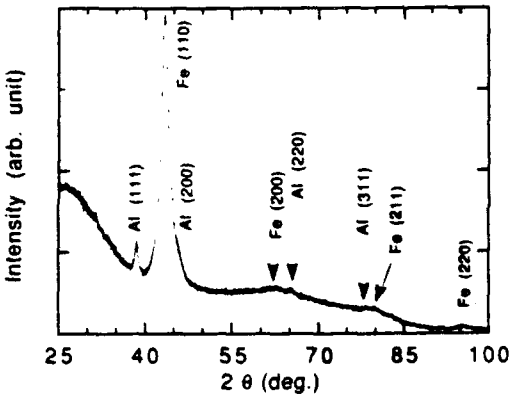

Fig. 2. 2θ X-ray diffraction pattern taken using Cu Kα radiation of an Al/Fe multilayer deposited without ion beam assistance.

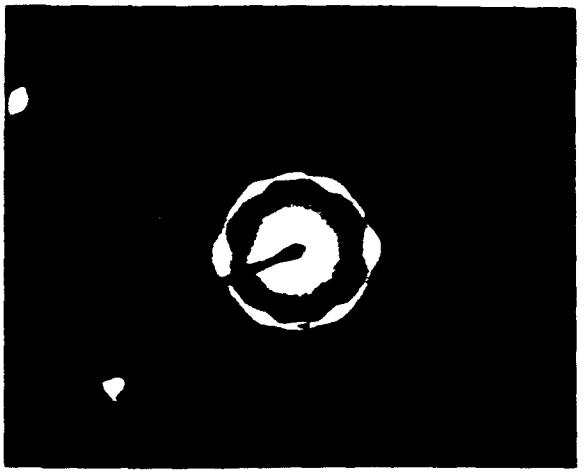

Fig. 3. Selected area electron diffraction of an Al/Fe (unassisted) multilayer film.

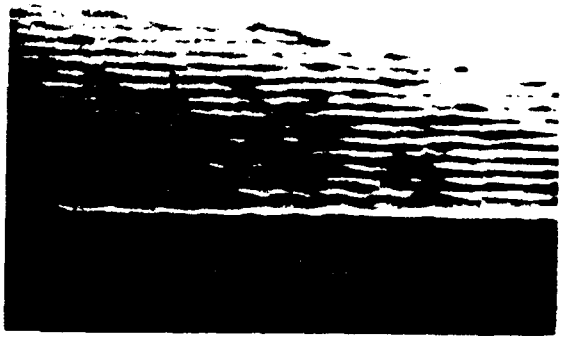

Fig. 4. Cross-sectional view of a TEM image of an Al/Fe (unassisted) modulated structure showing the periodic structure with a wavelength of 43 Å.

Nagakubo *et al.* [4] who observed a change in orientation from (110) to (200) as the iron layer thickness decreased from 200 Å to below 20 Å. The lattice parameter of aluminum in the present case is in very good agreement with its bulk value. In the case of ion beam assisted samples the peaks for Al(111) and Fe(110) were broad when compared with the non-assisted case.

Figure 3 shows the selected area electron diffraction of the unassisted sample. It is clear from this figure that the multilayer film is textured and has (110) orientation for b.c.c. ion. Figure 4 shows a bright-field TEM image from XTEM of the same sample. The incident beam direction is close to the [110] axis of the silicon substrate and parallel to the plane of the substrate-film interface. Since iron is denser and has a higher atomic number than aluminum, it scatters more strongly. Thus, the dark layers are iron and the lighter layers are aluminum. The wavelength obtained from XTEM was in very good agreement with the value obtained from small angle X-ray diffraction and fluorescence analysis, i.e. 43 Å. The other dark regions seen in this micrograph may be attributed to crystallites with different orientation [10].

3.2. Magnetic properties of Al/Fe multilayer films

The magnetic properties of the Al/Fe multilayer structures were observed using FMR at 10 GHz, and with a VSM. The VSM was used to determine the total moment of the sample from which the moment per volume of iron M was calculated. The out of plane field required for magnetic saturation using the VSM and

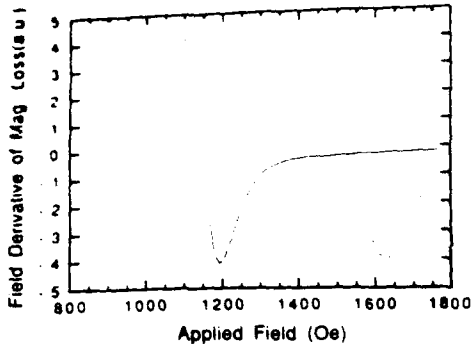

Fig. 5. Ferromagnetic resonance lineshapes measured at 10 GHz for fields applied in the sample plane. The ion beam assisted deposition is seen to produce a narrower line and a lower resonance field, indicative of higher M.

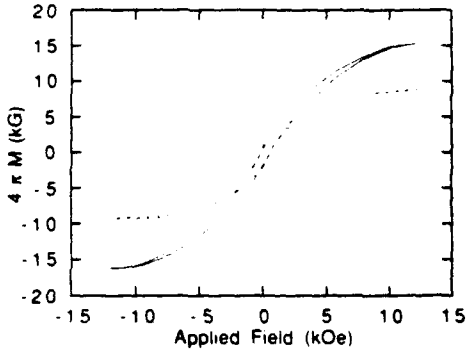

Fig. 6. Magnetic moment *vs.* applied field as measured by the VSM for fields perpendicular to the film plane, for Fe/Al multilayers made with and without ion beam assistance. The lower fields required for saturation compared with $4\pi M$ indicate that the out of plane (axial) direction is magnetically easy.

the effective magnetic moment as deduced from FMR indicate that there is moderate growth induced and surface or other magnetic anisotropy favoring the out of plane orientation in these samples.

FMR spectra of the two types of films are shown in Fig. 5. The lower field position and narrower linewidth of the sample made with ion beam assistance are indications of the higher moment and softer magnetic qualities achieved. Figures 6–8 show the VSM results for the two samples in three different orientations: perpendicular to the film plane, and in the film plane for the easy and hard directions. In addition to determining the total moment using the VSM, we find the fields required for saturation which indicate the magnetic anisotropies present along the measurement direction, substantiating the FMR results.

Magnetically, both samples have a well developed ferromagnetic moment, they have high permeabilities

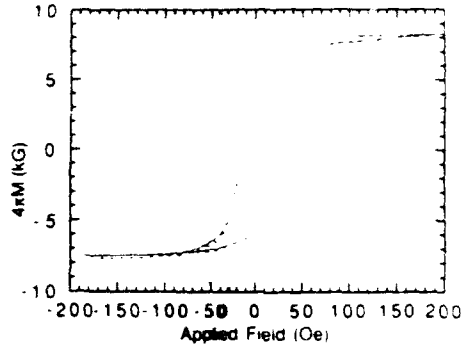

Fig. 7. Magnetic moment *vs.* applied field as measured by the VSM for fields in the film plane for films made without ion beam assistance.

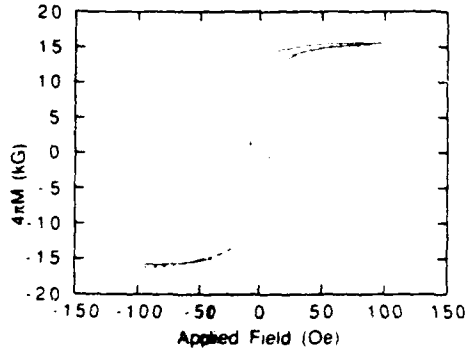

Fig. 8. Magnetic moment *vs.* applied field as measured by the VSM for fields in the film plane for films made with ion beam assistance. The higher magnetic quality of these films compared with those of Fig. 6 is evident.

for magnetic fields applied in the plane of the sample and they have low coercivities. However, the moments are reduced from those of bulk iron, especially for the case where the deposition was not ion beam assisted. A summary of the results is shown in Table 1, with the

TABLE 1. Comparison of magnetic properties of Fe/Al thin film multilayers

	Without ion beam assistance	With ion beam assistance	200 Å polycrystal
$4\pi M$(kG)	9.9	15.6	20
H_a(Oe)	15.0	6.0	3
H_c(Oe)	11.0	2.0	Few
Perpendicular magnetic anisotropy (KOe)	+3.0 (axial)	+6.0 (axial)	Small
FMR, 10 GHz linewidth (Oe)	180.0	100.0	25
Fe(thickness) for 100 layers (Å)	1330	1500	
Al (thickness) for 100 layers (Å)	2900	4500	

properties of thin polycrystalline iron films of thickness about 200 Å given for comparison (for this thickness range the surface and interfacial effects are expected to be an order of magnitude less important). The results obtained with ion assisted deposition are qualitatively similar to those of Nagakubo *et al.* [4] for comparable iron and aluminum thicknesses although we were able to obtain a somewhat lower coercivity.

4. Conclusions

X-ray diffraction results show that iron is in b.c.c. phase in Al/Fe multilayers grown by a dual-ion-beam deposition technique. The lattice parameter of iron is measured to be 2.94 Å and is enhanced when compared with its bulk value. Magnetically, iron films have a well developed ferromagnetic moment, high permeabilities for magnetic fields applied in the plane of the sample and low coercivities.

References

1 T. Shingo, N. Hosoito, K. Kawaguchi, T. Takada, Y. Endoh, Y. Ajiro and M. Friedt, *J. Phys. Soc. Jpn.*, 52 (1983) 3154.
2 Y. Kozono, M. Komuro, S. Narishige, M. Hanazono and Y. Sugita, *J. Appl. Phys.*, 61 (198) 4311.
3. Z. S. Shan, Z. R. Zhao and D. J. Sellmyer, *J. Appl. Phys.*, 61 (1987) 4320.
4 M. Nagakubo, T. Yamamoto and M. Naoe, *J. Appl. Phys.*, 64 (10) (1988) 5751.
5 B. Heinrich, Z. Celinski, J. F. Cochran, W. B. Muir, J. Rudd, Q. M. Zhong, A. S. Arrott, K. Myrtle and J. Kirschner, *Phys. Rev. Lett.*, 64 (6) (1990) 673.
6 D. A. Steigerwald and W. F. Egelhoff, Jr., *Surf. Sci.*, 192 (19) L877.
7 S. B. Qadri, C. Kim, K. H. Kim, P. Lubitz and M. Twigg, *J. Vac. Sci. Technol. A*, 9 (1991) 430.
8 S. B. Qadri, C. Kim, M. Twigg, P. Lubitz and M. Rubinstein, *J. Vac. Sci. Technol. A*, 9 (1991) 512.
9 C. Kim, S. B. Qadri, H. Y. Yu, K. H. Kim, B. Maruyama and A. S. Edelstein, *J. Vac. Sci. Technol. A*, 8 (3) (1990) 1407.
10 C. Kim, S. B. Qadri, M. Twigg and A. S. Edelstein, *J. Vac. Sci. Technol. A*, 8 (1990) 3466.

Quantum size effect and the giant magnetoresistance in magnetic multilayers

A. C. Ehrlich and D. J. Gillespie
U. S. Naval Research Laboratory, Washington, D. C. 20375

A theoretical model which accounts for the variations of the giant magnetoresistance, $\Delta\rho/\rho$, with electron mean free path, L, interface roughness, r, and magnetic, t_M, and normal layer, t_N, thickness has been previously presented for sandwich films. It employs the quantum-size-effect theory of resistivity in thin films and relies on spin dependent transmission or reflection at individual layer boundaries to establish the metallic quantum-well states. This model has now been extended (i) to films where L can be different in the magnetic, L_M, and nonmagnetic, L_N, layers, (ii) to an electron/atom number, n, of 0.131 as well as 1.047, and (iii) to films from sandwiches to those with as many as 64 (63) magnetic (nonmagnetic) layers. The focus is on films with relatively thin t_M and t_N where quantum, as distinguished from semiclassical, effects should dominate. Typical results can be summarized as follows: for $t_M \sim t_N \sim 10$ monolayers, ML, and L's ~ 70 ML, $\Delta\rho/\rho$ increases more rapidly as L_M than L_N but this effect is reduced as one goes from sandwiches to superlattices; $\Delta\rho/\rho$ is approximately 50% in a superlattice with $r=5$ ML, which is an order of magnitude larger than in a superlattice with $r=1$ ML. In a sandwich the difference between $r=5$ and $r=1$ is closer to a factor of 5. In the sandwiches $\Delta\rho/\rho$ is smaller for $n=0.131$ than for $n=1.05$.

I. INTRODUCTION AND BACKGROUND

Recently one of the authors[1] of this paper presented a theoretical model which can account for the experimentally observed variations of the "giant magnetoresistance" (GM) with mean free path L, interface roughness r, magnetic layer thickness t_M, and normal (nonmagnetic) layer thickness t_N. Further, by its very nature it is clear that it predicts a much larger effect for multilayers than for sandwiches which is also observed. The numerical calculations that were presented have been limited to sandwiches with one conduction electron/atom and to the assumption that the bulk material electron mean free path was the same in both the magnetic and normal layers. In this paper the numerical calculations are extended to multilayers with up to 64 magnetic layers (superlattices) and to systems where the mean free path is different in the magnetic and normal layers.

The essential ideas underlying the physical mechanism in Ref. 1 and this paper are as follows: the majority spin s^+, and minority spin s^-, of the magnetic material M, have distinctly different band structures. For the nonmagnetic material N, the electron's s^+ and s^- distinguishes only the spin direction in space. We hypothesize that one of the spin bands in M, say the s^- band, has a band structure very similar to that of the N electrons, as is the case, e.g., in Fe and Cr,[2] whereas the s^+ band structure of M is very different. In these circumstances at the M-N interfaces, the s^- electrons will be much more transmissive and much less reflective than will the s^+ electrons. In Ref. 1 and for this semiquantitative work we make two simplifying assumptions; (i) we take the s^- electrons to be perfectly transmissive and the s^+ electrons perfectly reflecting at the M-N interface, (ii) we use the spherical band model for all bands.

The experimental situation is shown in Fig. 1 with Fig. 1(a) illustrating antiferromagnetic and Fig. 1(b) the ferromagnetic spin orientation of the M layers in a multilayer. With the assumptions of the previous paragraph the electrons grouped by the dashed circles see no M-N interface that is between them but are totally reflected by an interface outside the grouping. Thus these grouped regions constitute metallic quantum wells. There is ample evidence in the recent literature from angle-resolved photoemission spectroscopy[3-5] and inverse photoemission spectroscopy[6] for the existence of these wells in metallic systems. Therefore, ignoring for the moment any electric current that might be carried by the s^+ electrons in the M layers, Fig. 1(a) represents m-2 parallel conducting quantum wells of thickness $2t_N + t_M$, where m is the number of M layers and two wells of thickness $t_N + t_M$. Figure 1(b) has one well of thickness $mt_M + (m-1)t_N$ and $(m-1)$ wells of thickness t_N. An analogous argument can be made for sandwiches.

The conductivity of each of these quantum wells can be obtained from the quantum transport size-effect theory of Trivedi and Ashcroft.[7] The total conductivity of the multilayer of Fig. 1(a), for example, will be different from that of Fig. 1(b) because the thicknesses are different, and thus the consequences of size effect are different. This difference constitutes a major contribution to the giant magnetoresistance of sandwiches and higher number multilayers. To the extent that the s^+ electrons in the M layers do conduct, their conductivity will be the same in the magnetic configuration shown in Fig. 1(a) as in Fig. 1(b), and thus will diminish the magnitude of the magnetoresistance but not alter qualitatively the effect of this mechanism.

II. EFFECTIVE MEAN FREE PATH IN A MULTILAYER QUANTUM WELL

Consider a thin bilayer film in which the mean free path differs appreciably in the two layers but in which there is no reflection at the interface between the two layers. For example, a 99.999% pure Cu single crystal layer

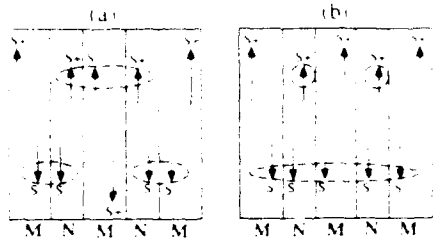

FIG. 1. The spin structure of multilayer films with nonmagnetic, N, layers between identical magnetic layers, M. In M, + and − refer to majority and minority spin bands respectively and ↑ and ↓ are the spin directions in space. In N, + ≡ ↑ and − ≡ ↓. a and b illustrate antiferromagnetically and ferromagnetically oriented M layers, respectively. The dashed circles group electrons that constitute a single quantum well.

grown epitaxially on a 99.9% Cu layer and studied at low temperature. If the film is sufficiently thin in the z direction then the wave functions would be quantized to the thickness of the film in the z direction and would all extend fully across both layers of the film. An electron carrying current in the x direction, say, would encounter the impurities in the two layers on an equal footing. The "effective mean free path in the bulk," a parameter needed in the Trivedi and Ashcroft theory, is essentially the reciprocal of a thickness weighted average of the scattering rate in each of the two layers and can easily be shown to be

$$L=\frac{(t_1+t_2)L_1L_2}{t_2L_1+t_1L_2}, \tag{1}$$

where L_1 and L_2 are the mean free paths in layers 1 and 2, respectively, and t_1 and t_2 are the corresponding thicknesses.

The implications of this quantum picture of electrons in a multilayer are somewhat different than those obtained from the semiclassical wave packet picture for the conduction electrons. Most important, one cannot think of separate mean free paths within each layer of the film, although the concept of a bulk mean free path (essentially the reciprocal of the scattering rate divided by the Fermi velocity) that is representative of each of the materials is still valid. Thus it is also not meaningful to think of a tendency for the more highly conductive layer to short out the less conductive layer in this more exact quantum picture. Of course, the layers must be thin enough and the interfaces transparent to the wave function (coherent wave function across the film) for this quantum picture to hold.

The interplay between the scattering rate in quantum multilayer systems implicit in Eq. (1) and the different combinations of layers and layer thicknesses in Figs. 1(a) and 1(b) that make up the quantum wells can have surprising consequences. Given different values of the two thicknesses, t_M, t_N, and the two mean free paths, L_M, L_N, one would find a magnetoresistance, i.e., a difference in resistance, between the magnetic configurations of Figs. 1(a) and 1(b), even excluding the quantum size effect. This statement is, of course, hypothetical in that a conducting layer thin enough to be in the quantum regime will also be effected by quantum size effect.

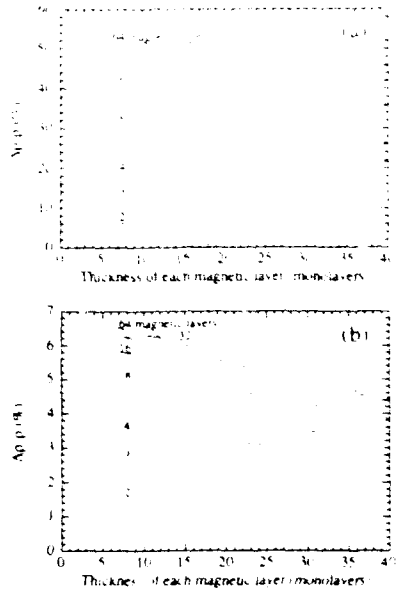

FIG. 2. The calculated GM vs t_M for the indicated number of magnetic layers. There is always one fewer nonmagnetic layer. t_N is fixed at 10 ML. $L_M=L_N=70$ and $n=1.047$. In a, $r=5$ whereas in b, $r=1$.

III. RESULTS

In this paper all the calculations are for multilayers in which the number of M layers exceeds the number of N layers by one. Figures 2(a) and 2(b) show the results of a calculation of $[\rho(0)-\rho(B)]/\rho(0)=\Delta\rho/\rho$ (the negative of the usual magnetoresistance) for approximately 1 conduction electron/atom ($n=1.047$) and 10 monolayers (ML) in the nonmagnetic layer (all dimensions will be given in ML) as a function of magnetic layer thickness for various number of magnetic layers in a superlattice. Values for r, L_M, and L_N are given in the figure caption. Figures 3(a) and 3(b) are for identical values of the parameters except that $n=0.131$ electrons/atom.

In Figs. 2 and 3 the mean free paths are taken to be identical in both materials at a middling 70 ML in order to isolate a number of features of this model of the GM. As expected, multilayers give an increasingly higher effect as the number of layers increases, other parameters held constant, with the expected tendency toward saturation. Figures 2 and 3 also illustrate the important effect of roughness. We have taken $r=1$ and $r=5$ ML, very little and very much roughness, which should, therefore, bracket any real world roughness likely to be found. For $n=1.047$, Fig. 2, the GM increases by a factor of $\simeq 3$–4 with the change in roughness for a range of layer numbers. There is a slightly slower approach to saturation with increasing layer number in the rougher sample. For $n=0.131$ and $r=5$, Fig. 3, the GM is reduced by a factor $\simeq 2$ compared to $n=1.047$ and $r=5$ but by a factor of 20 when comparing for $r=1$; that is, there is a difference of a factor of $\simeq 100$ for the two roughnesses when $n=0.131$. The primary reason for this is that surface roughness generates the greatest change in

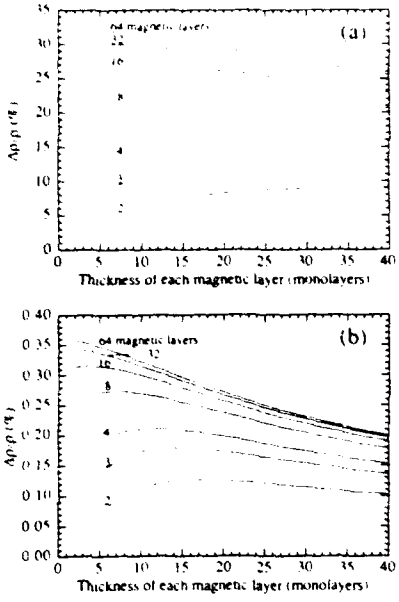

FIG. 3. Same as Fig. 2 except that $n=0.131$.

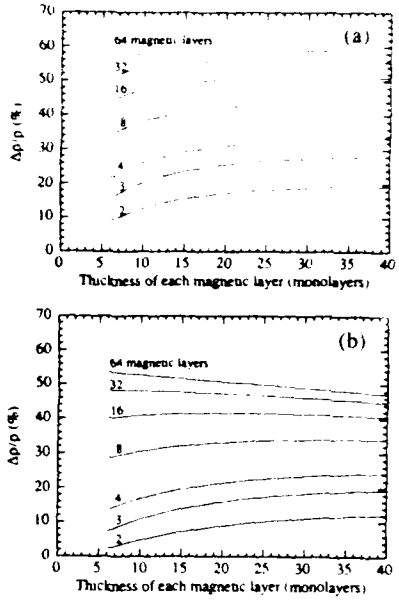

FIG. 4. Same as Fig. 2 except (a) $L_M=140$, $L_N=70$ and $r=5$ and (b) $L_M=70$, $L_N=140$ and $r=5$.

resistivity with size in the Trivedi and Ashcroft[7] theory but this falls off not only with reduced roughness but with reduced electron concentration.

Figure 4 addresses the issue of different mean free paths. Note the qualitative difference between films with a large number of layers depending on whether the M or the N layer has the longer mean free path. If L's of 30 and 70 were shown instead of 70 and 140, the results would appear qualitatively the same and would quantitatively differ by only $\approx 20\%$ (smaller). It is interesting to note that if large $\Delta\rho/\rho$ are sought, it is more advantageous to increase L_M than L_N. For very small size effect due to relatively smooth surfaces, say $r=1$, and particularly if also $n=0.131$, the calculation is dominated by the effects of the interplay of the mean free paths and the quantum well thicknesses discussed above. This leads to small values of $\Delta\rho/\rho$ and if $L_N > L_M$ and there are very few ML of M, even negative values.

In conclusion, the theoretical model of Ref. 1 has been extended to physical situations not previously treated. Superlattices are generally found to have a GM $\approx$ 4–10 times larger than comparable sandwiches, in general agreement with experiment. The general variation of the GM with r, n, t_M, and t_N (although not discussed here for lack of space) is qualitatively the same as predicted by the model for sandwiches[1] and is also in agreement with experiment. To achieve large GMs it is more important to have longer L_M's than L_N's.

[1] A. C. Ehrlich (unpublished), see also Bull. Am. Phys. Soc. **37**, 198 (1992).
[2] J. Inoue, A. Oguri, and S. Maekawa, J. Phys. Soc. Jpn. **60**, 376 (1991); K. B. Hathaway (private communication).
[3] T. Miller, A. Samsavar, G. E. Franklin, and T. C. Chiang, Phys. Rev. Lett. **61**, 1404 (1988).
[4] M. A. Mueller, A. Samsavar, T. Miller, and T. C. Chiang, Phys. Rev. B **40**, 5845 (1989).
[5] S. A. Lindgren and L. Wallden, Phys. Rev. Lett. **61**, 2894 (1988); Phys. Rev. B **38**, 3060 (1988); Phys. Rev. Lett. **59**, 3003 (1987).
[6] F. J. Himpsel, Phys. Rev. B **44**, 5966 (1989).
[7] N. Trivedi and N. W. Ashcroft, Phys. Rev. B **38**, 12 298 (1988).